

# Ultrasonographic Differentiation of Lateral Elbow Pain

## Authors

R. Obuchowicz<sup>1</sup>, M. Bonczar<sup>2</sup>

## Affiliations

<sup>1</sup>Radiology, Jagiellonian University, Krakow, Poland

<sup>2</sup>Surgery, Intermed, Krakow, Poland

## Key words

- elbow
- ultrasound
- pain
- lateral

## Abstract



Lateral elbow pain is often attributed to degenerative or posttraumatic impairment of the common extensor tendon. Ultrasonography assesses the soft tissue structures of the lateral elbow, allowing the differentiation between various underlying processes, including angiofibroblastic degeneration, hyaline degeneration, and inflammation, and exclusion of other possible causes of pain such as posterior interosseous and lateral antebrachial nerve compression. Furthermore,

the real-time imaging nature of ultrasonography enables the detection of impingement of the lateral synovial fold, degenerative changes in the elbow recess, and elbow posterolateral instability during dynamic maneuvers. Ultrasonography is widely accessible and well tolerated by patients, making it a perfect method for establishing an initial diagnosis and monitoring the healing process. This review describes the possible causes of lateral elbow pain and their ultrasonographic differentiation.

## Introduction



Lateral elbow pain is a potentially debilitating condition affecting both sports and daily life activities. In severe cases it may also disturb sleep. This very common disorder occurs not only in athletes but also often in office workers, and a strong association with trauma and hard labor has been noted [1,2]. Although in clinical practice lateral elbow pain is habitually attributed to the common extensor tendon impairment referred to as lateral epicondylitis, possible causes are numerous and can include degeneration and trauma of the lateral ligament components, posterior interosseous nerve (PIN) entrapment, lateral antebrachial cutaneous nerve entrapment, posterolateral synovial fold impingement, postero-lateral elbow instability, and radiocapitellar joint osteoarthritis [3]. Therefore, lateral pain of the elbow can present a challenging diagnostic dilemma, and adequate diagnosis is important because treatment approaches vary according to causative factors. For instance, rehabilitation therapy is appropriate if the lateral elbow pain is caused by tendinopathy of the common extensor tendon or mild PIN neuropathy, whereas full-thickness tears of

the tendons or high-grade PIN neuropathy may require surgical treatment [4].

Ultrasonography enables the assessment of soft tissue structures as well as the cortical surface of bones. The effectiveness and affordability of this method make it a perfect tool not only for disease detection but also for monitoring the healing process. Furthermore, the extent of the disease and its severity can be easily revealed. The elbow joint is relatively small, and numerous complex anatomic structures with variable orientations are closely positioned in this region. In this regard, the high spatial resolution of modern ultrasound devices and the ability to quickly select and adjust the imaging plane during the scan are of great practical importance [5,6]. Moreover, real-time dynamic ultrasonography provides a principle advantage by allowing the functional assessment of tendons and ligaments [7]. Below we describe various anatomical aspects of pathologies that can cause lateral elbow pain and their differentiation using high-resolution ultrasonography.

received 05.07.2015

accepted 07.02.2016

## Bibliography

DOI <http://dx.doi.org/10.1055/s-0035-1569455>  
 Ultrasound International Open  
 2016; 2: E38–E46  
 © Georg Thieme Verlag KG  
 Stuttgart · New York  
 ISSN 2199-7152

## Correspondence

R. Obuchowicz, PhD  
 Jagiellonian University  
 Radiology  
 Kopernika 19  
 Krakow  
 Poland 31-051  
 Tel.: +48/661/117 736  
 r.obuchowicz@gmail.com

## License terms



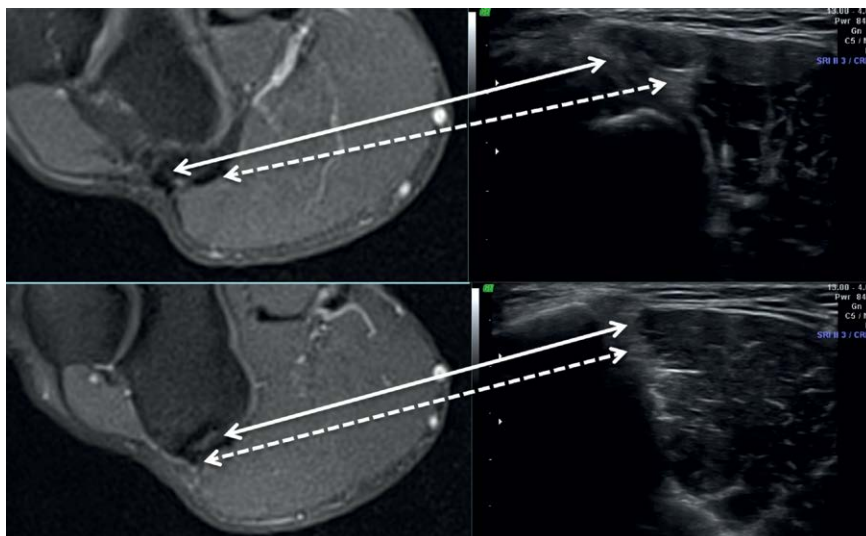


**Fig. 1** The common extensor tendon at the level of the lateral humeral epicondyle, top image shows proximal scan and bottom image presents a distal scan. Figure presents a comparison of an axial sonogram (linear array probe, 6–12 MHz SP GE [Voluson 730 Expert]) (right) with a proton-density magnetic resonance image with fat saturation, axial plane (1.5 T, Magnetom Essenza) (left). The dashed arrows indicate the extensor digitorum communis (EDC), whereas the solid arrows point to the extensor carpi radialis brevis tendon (ECRB). The hyperechoic areas on sonographic image and low signal areas on MR images represent intact collagenous structures; the EDC and ECRB contribute to the formation of the superficial and deep layers of the “common” extensor tendon, respectively.

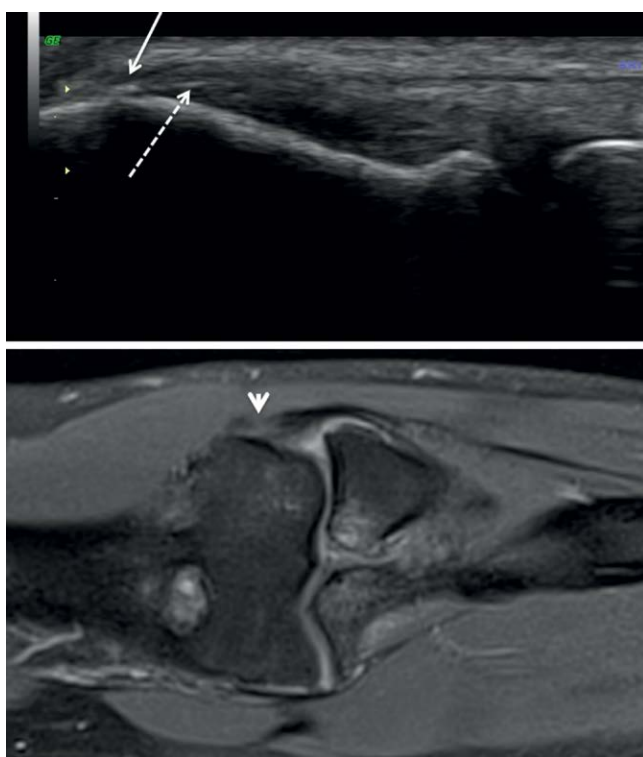


**Fig. 2** Early degenerative changes of the common extensor tendon at the level of the lateral humeral epicondyle: a comparison of a magnetic resonance scan (proton density with fat saturation, coronal plane, 1.5 T Magnetom Essenza) (bottom) with a sagittal sonogram (linear array probe, 6–12 MHz SP GE [Voluson 730 Expert]) (top). The common extensor tendon lies laterally to the collateral ligament (these structures are fused proximally at the level of the enthesis). The ligament/bone interface at the level of the enthesis is irregular (solid arrow) because of calcification, with no formed enthesophytes. A small scar in the deep part of the attachment is visible (dashed arrow). These early changes are not visible in magnetic resonance imaging because the signal intensity is similar to that of collagen (site of attachment is indicated by arrowhead).

### Assessment of Lateral Epicondylitis

The common extensor tendon attached to the anterior aspect of the lateral epicondyle and lateral supracondylar ridge consists of conjoined tendons of the extensor digitorum communis (EDC) – the extensor digiti minimi and supinator – which merge their

fibers with the extensor carpi radialis brevis (ECRB), while the extensor carpi ulnaris merges with EDC. The epicondylar attachment of the ECRB and EDC consists of 2 layers: the deep layer composed mainly of ECRB fibers, and the superficial layer formed by the EDC (● Fig. 1). ECRB has additional origins from various structures, including the lateral collateral ligament (LCL), annular ligament, and intramuscular septum. The tendon lies immediately over the LCL, and these 2 structures are interconnected by crossing fibers and are related both morphologically and functionally [8]. The distal fibers contribution from the muscle bellies can be traced and separated. The lateral tendoligamentous complex at the level of the elbow is easily accessible to ultrasonographic examination because it is located immediately under the subcutaneous tissue and the fascia. Normally, the complex is visualized as a hyperechoic linear structure aligned between the corresponding attachments.

Microtrauma caused by the overuse of the hand results in local rupture of individual fibers, predominantly in the area of the deep part of the common extensor tendon attachment, namely, ECRB. Spontaneous healing of multiple repeated microtears alters the tendon composition by replacing collagen fibers with reparatory scar tissue, whose structure differs from that of the normal tendon [9] (● Fig. 2). The main component of this tissue is numerous atypical fibroblasts of a mesenchymal origin, which form a proteinaceous matrix. As a result, normal fibrillar collagen is replaced with disorganized amorphous collagen [10]. The third component of tendinosis is inefficient vascularization characterized by immature endothelial cells and no functional vascular lumen. Because of the lack of effective blood supply, the amorphous tissue is devoid of macrophages and neutrophils and has no healing potential; therefore, no signs of inflammation can be found [11,12]. Ultrasonographic detection of such areas is based on the lack of normal reflectivity of collagen fibrils, non-reflective amorphous tissue is visible as an anechoic region. Anisotropy always has to be taken into consideration when scanning the tendon. Limited or absent reflectivity of collagen tissue may also occur in cases with partial and complete rupture of collagen fibrils. Although differentiation of tears vs. tendinosis using ultrasonography may be challenging sometimes, it should be based on the general rule that tendinosis presents in US as tendon hypoechogenicity and thickening of the tendon, whereas a tear is typically hypoechoic or anechoic and is associated with tendon volume loss [13] (● Fig. 3,4).

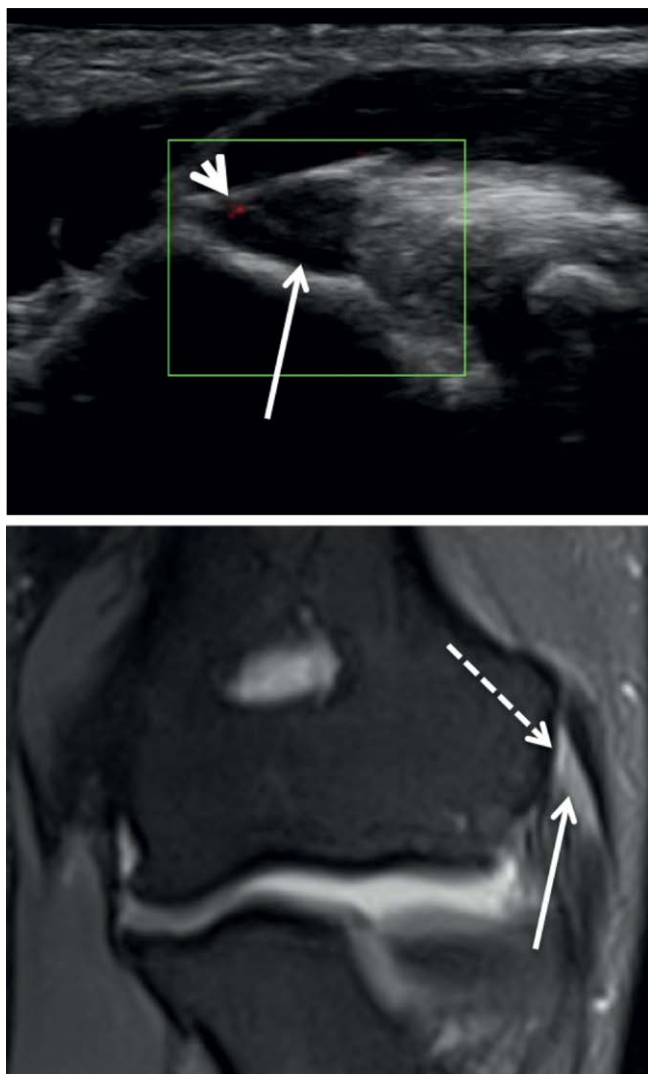


**Fig. 3** Advanced degenerative changes of the common extensor tendon at the level of the lateral humeral epicondyle: a comparison of axial and sagittal sonograms (linear array probe, 6–12 MHz SP GE [Voluson 730 Expert]) (top) with a magnetic resonance (MR) image (proton density with fat saturation, coronal plane, 1.5 T Magnetom Essenza) (bottom). The hypoechogenicity of the layers on the sagittal sonogram (solid arrow) with its thickening. Note the single vessel (arrowhead) within the area of degeneration with no signs of inflammation. On Doppler, there is only a single vessel detected adjacent to the bony entheses. The MR image reveals the irregularity of the tendon and high-intensity signal, suggesting decomposition of the collagen structure (solid arrow). No major degenerative changes are present at the level of the bony entheses (dashed arrow).

It has been suggested on the basis of experience that tendinosis is usually confined to the deep layer of the epicondylar attachment (ECRB), specifically to the region within 1/3 of it [14]. Inflammation, which represents a reparatory reaction, may lead to tendon hypoechogenicity due to edema and exudative fluid presence at the site of attachment and along the collagen bundles. Infiltration of inflammatory cells and production of cytokines with secondary neovascularization are responsible for this process [15]. The use of the power Doppler option present in all modern ultrasound machines allows for visualization and detection of blood flow (◊ Fig. 5). This very sensitive technique

allows for monitoring of the healing process after PRP (platelet rich plasma) injection but also can help in differentiating early stages of tendinosis (where some inflammatory cells may be present) from sites of rupture where no vascular tissue is found. It is equally useful for monitoring outcomes after other treatment options such as dry needling, Hyaluronic acid injection, or dextrose prolotherapy [16]. Steroid injections in the absence of inflammation are not supposed to be considered for therapy.

### Assessment of PIN Entrapment

PIN neuropathy can be confused with extensor attachment tendinosis because the clinical symptoms, as well as the location and severity of pain, are often alike. Patients with PIN neuropathy typically present with lateral elbow pain, which sometimes radiates along the course of the nerve [17]. The PIN is a mixed motor and sensory nerve with the motor component extending to the extensor muscles group. The nerve also includes unmyelinated (IV) sensory fibers from the radioulnar and radiocarpal joint capsules [18]. The predominant compression site of the PIN is the arcade of Frohse, a fibrous arch formed by the proximal edge of the superficial head of the supinator muscle [19] (◊ Fig. 6). However, the PIN may be compressed at multiple sites, of which the most important are the fibrous band between the brachioradialis muscle and the brachialis, recurrent radial vessels, and the proximal edge of the ECRB [20]. In the surgical community, the deep (motor) branch of the radial nerve referred to as the PIN includes the region from the site of the radial nerve bifurcation throughout the whole radial canal, namely, from the radiohumeral joint plane to the distal edge of the supinator muscle [21]. Anatomical determinants such as thickened tendinous fascia forming a fibrous arcade in the radial canal can result in high pressure on the PIN. Thus, during maximum active contraction, the peak pressure may reach 190 mm Hg, whereas ischemia of the nerve can occur at a pressure of 60 mm Hg [22,23]. Chronic irritation of the nerve with mechanical impingement and ischemia-reperfusion cycles may induce fibrillar degeneration of the fascicles and perineural fibrosis, contributing to formation of a neuroma.

If PIN degeneration is suspected, meticulous scanning of the radial canal region with a high-resolution probe (up to 16 MHz) is mandatory [24]. The anteroposterior diameter of a normal nerve in the radial tunnel and supinator canal does not exceed 1 mm [25], and the site of PIN compression can be detected based on an increase of this diameter in the region of the neuroma. This should not be confused with the slight increase in the PIN diameter proximally to the arcade of Frohse and variations that may occur because of normal changes of the course of the nerve [26] (◊ Fig. 7). Although the most common site of compression and therefore neuroma detection is at the level of the arcade of Frohse, neuromas can also occur at other sites, such as the recurrent radial artery and the medial edge of the ECRB [27]. Other less frequent causative factors of PIN palsy include tumors (usually lipomas or neuromas) located on the course of the main trunk or branches of the nerve. Differentiation of the exact location of the tumor is important as lesions of the main trunk and branches are treated differently (◊ Fig. 8).



**Fig. 4** A tear of the deep part of the common extensor tendon at the level of the lateral humeral epicondyle: a comparison of axial and sagittal (enlarged field of interest) sonograms (linear array probe, 6–12 MHz SP GE [Voluson 730 Expert]) (top) with magnetic resonance (MR) images (proton density with fat saturation, coronal and axial planes, 1.5T Magnetom Essenza) (bottom). Rupture of the fibers of the common extensor tendon is visible on the sagittal sonogram as the uniformly dark area marked with calipers on the sagittal and axial sonogram. Areas with no reflection from collagen fibrils is depicted by solid arrows. Note also the decreased thickness of the tendon. In the corresponding MR image, the bright signal corresponding to the fluid and the lack of signal from the collagen fibrils can be noted in the deep layer of the common extensor tendon (solid arrow).



**Fig. 5** Inflammation of the common extensor tendon at the level of the lateral humeral epicondyle: a comparison of axial and sagittal sonograms (power Doppler mode, linear array probe, 6–10 MHz SP GE [Voluson 730 Expert]) (top) with magnetic resonance (MR) images (T1-weighted spin-echo sequence with fat saturation, axial plane, 1.5T Magnetom Essenza) (bottom). Increased vascularization is colored in the power Doppler mode in the sagittal sonograms (solid arrow). In the corresponding axial MR image, the bright signal from the tendon can be noted after intravenous contrast infusion (dashed arrow). Note the differences in signal intensity between pre- and post contrast images.

### Assessment of the Lateral Ligamentous Complex

Injury of the lateral collateral ligaments (LCL) can be another important cause of lateral pain in the elbow. Ultrasonography (US) seems to be the most useful technique both for the diagnosis of LCL injury and for monitoring the healing process of its components. In addition, US allows real-time evaluation of the injured LCL in motion (varus test and flexion-extension). The anatomy of the LCL is complex because of the presence of several interconnected bundles as well as anatomical variability [28,29]. Its components are, namely, the radial collateral ligament proper (RCL), annular ligament (AL), and lateral ulnar collateral ligament (LUCL). Biomechanically, the LCL components are among the most important stabilizers of the elbow and can be injured to different extents, usually during a fall on an outstretched hand, as described by O'Driscoll et al. [30]. The lateral ulnar collateral ligament is especially important in this regard as it is the primary stabilizer against posterolateral rotatory instability [31], which may cause painful or painless clicking of an otherwise asymptomatic elbow. The components of the LCL can be evaluated by static ultrasonography as well as during real-time dynamic maneuvers [32] (● Fig. 9). Meticulous dynamic and morphologic assessment of all the bundles of the LCL complex facilitates clinical decision making when devising treatments for posttraumatic lateral elbow.

### Assessment of Posterolateral Plica Syndrome

Elbow synovial fold syndrome is recognized as a frequent cause of lateral elbow pain in athletes [33] as well as in the general population [34]. The synovial fold is a structure continuous with the radiocapitellar joint capsule connected to the annular ligament, which has been proposed to act as an elbow joint stabilizer [35]. It may include continuous posterolateral, lateral, anterior, and lateral olecranon compartments differentiated according to their location. Posterolateral and anterior folds are the most prevalent, with lateral folds being the least common [36]. If irritated, lateral, posterolateral, and lateral olecranon synovial folds (if present) could be a source of lateral elbow pain (● Fig. 10). Fold irritation may be due to its compression by the bony structures (the capitellum and the outer edge of the radial dome) for lateral folds, the transverse sulcus of the sigmoid cavity and the radial dome for posterolateral synovial folds, and the lateral margin of the olecranon for lateral olecranon synovial folds. Repetitive compression induces an inflammatory reaction with edema and ultimately fibrosis, with a secondary increase of the volume of the fold. Enlarged synovial folds might be painful, and are prone to compression by the bony structures. Dislocation of a fold with painful snapping of the joint can be provoked and diagnosed during dynamic maneuvers (flexion and extension) (● Fig. 11).



## Assessment of the Lateral Antebrachial Cutaneous Nerve (LABCN)

LABCN injury is a possible cause of radial elbow pain. The LABCN is a sensory terminal branch of the musculocutaneous nerve situated in the cubital fossa close to the cephalic vein in the subcutaneous fat. Tingling, radiating burning pain, paresthesia in the anterolateral region of the forearm, and a positive Tinel's sign laterally to the biceps tendon are frequent manifestations of LABCN lesions [37].

Direct trauma, compression by an edema accompanying a biceps brachii lesion, and nerve entrapment under the biceps tendon

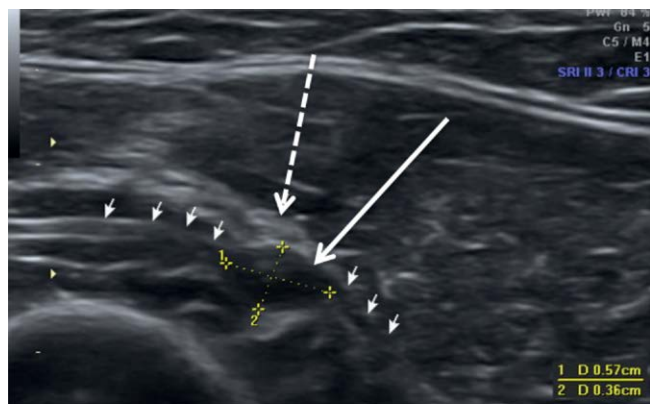


**Fig. 6** Neuroma of the posterior interosseous nerve due to compression by the arcade of Frohse. Sagittal sonogram of the posterior interosseous nerve in the proximal part of the supinator muscle (linear array probe, 6–12 MHz SP GE [Voluson 730 Expert]). The sagittal sonogram (top) shows neuroma borders (indicated by the calipers). The small white arrows indicate the proximal and distal courses of the nerve. The large solid arrows show the neuroma. The dashed arrows show the thickened arcade of Frohse. Intraoperative dissection (bottom) revealed the thickened nerve and arcade of Frohse (cut).

during pronation/extension of the arm are possible causes of nerve compression [38]. Moreover, injuries of the nerve may be caused iatrogenically during vein puncture and phlebotomy [39]. Radiation of the pain distally and radially may mimic lesions of the lateral part of the elbow joint, and therefore precise identification of the nerve location and a meticulous search for possible lesions are compulsory.

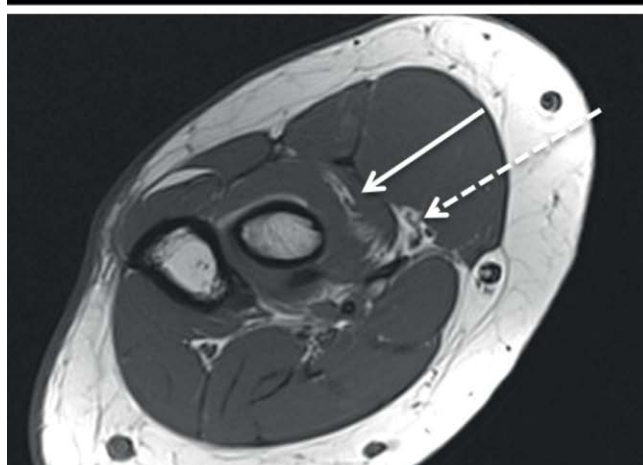
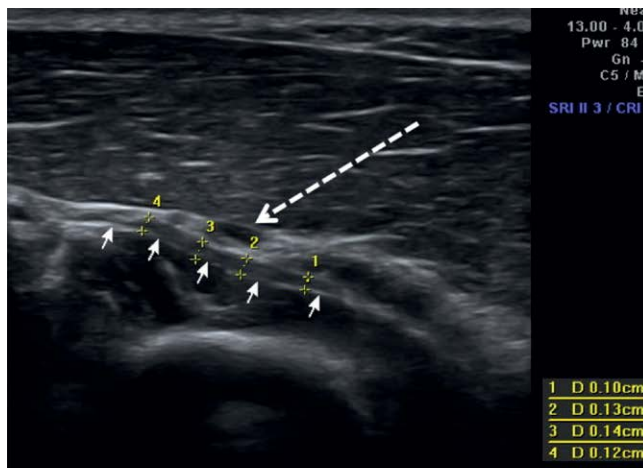


**Fig. 7** The course of the posterior interosseous nerve (PIN) in the proximal part of the supinator canal. The nerve is indicated by small arrows on the sagittal sonogram showing the proximal part of the supinator muscle (linear array probe, 6–12 MHz SP GE [Voluson 730 Expert]) (top). Comparison with a magnetic resonance (MR) image (T1-weighted spin-echo sequence, axial plane, 1.5T Magnetom Essenza) (bottom). The sagittal sonogram reveals a posterior interosseous nerve with normal diameter (indicated by the calipers in the sonograms and the solid arrow in the MR image). The proximity of the recurrent radial vessels (dashed arrow) may lead to nerve irritation and may induce lateral elbow pain. In the axial MR image, the PIN is clearly visible in the proximal part of the supinator canal (solid arrow). Note the prominent radial vessels (dashed arrows).

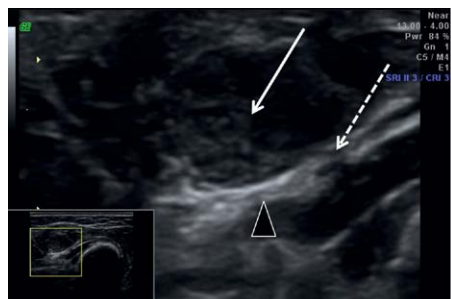


**Fig. 8** Lipoma of the posterior interosseous nerve (PIN) in the proximal part of the supinator canal. A sagittal sonogram of the PIN (enlarged picture) in the proximal part of the supinator muscle (linear array probe, 6–12 MHz SP GE [Voluson 730 Expert]) (left). Notice the connection of the tumor with the first branch of the nerve (dashed arrow) in the sagittal sonogram. The arrowhead depicts the main trunk of the PIN. Intraoperatively, the lipoma (solid arrow) was found close to the superficial part of the supinator muscle.

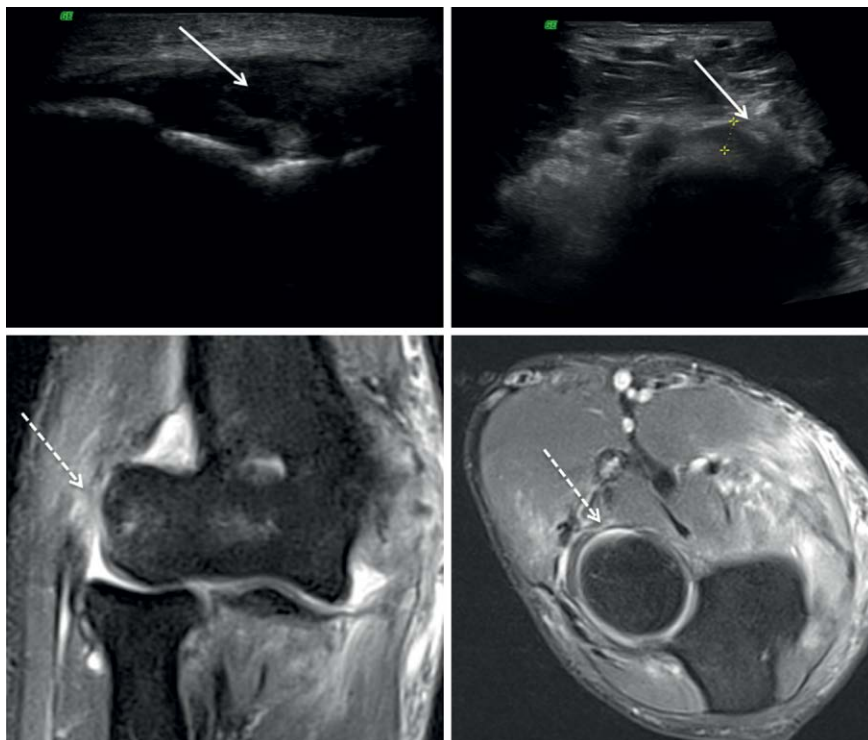


**Fig. 9** Injury of the components of the lateral collateral ligament visualized by sonography (top) and magnetic resonance (MR) imaging (bottom). Sagittal sonograms of the annular ligament, proper collateral ligament, and lateral ulnar ligament (enlarged image) in the proximal part of the supinator muscle (linear array probe, 6–12 MHz SP GE [Voluson 730 Expert]) are compared with MR images (T1-weighted spin-echo sequence, axial plane, 1.5 T Magnetom Essenza). The solid and dashed arrows indicate the injured lateral collateral ligament and annular ligament in the ultrasonography and MR images, respectively. The thickened annular ligament is depicted in the sonograms with the calipers.

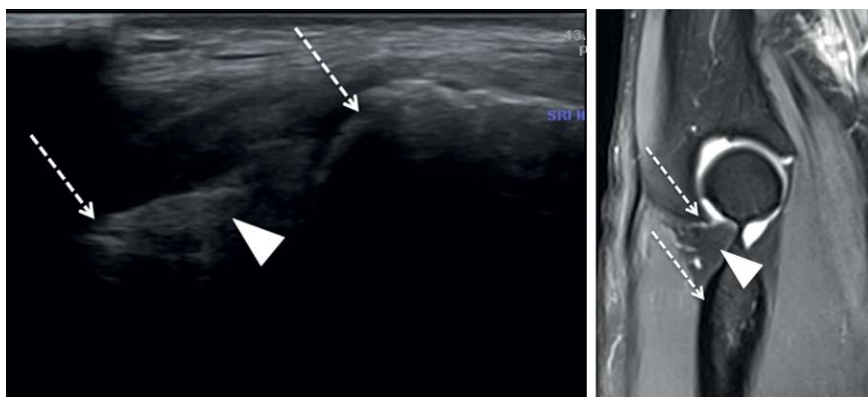


**Fig. 10** Overgrowth of the lateral olecranon synovial fold. A sonogram of the fold (sagittal oblique plane, linear array probe, 6–12 MHz SP GE [Voluson 730 Expert]) (top) and Magnetic resonance images (1.5 T Magnetom Essenza) (bottom) of a symptomatic overgrown fold (proton density with fat saturation sequence, sagittal plane). The folds are marked with the arrowheads. Arrowhead shows the hypertrophied fold (on MR and US image). The dashed arrows depict the bony margins of the olecranon and the olecranon fossa potentially conflicting with the fold.

Proximally to the elbow, the LABCN emerges from the lateral outline of the biceps brachii muscle to course epifascially close to the cephalic vein (◉ Fig. 12). This superficial location, which has been well documented in cadaveric studies utilizing ultrasonography, allows its reproducible recognition [40]. Accordingly, this nerve is easily accessible to ultrasonographic examination, making it a fast and reliable method for visualizing the nerves [41].

### Assessment of Posterolateral Rotatory Instability (PLRI)

PLRI of the elbow is a possible cause of lateral elbow pain, often mimicking lateral epicondylitis. PLRI is a term introduced by O'Driscoll and colleagues that refers to the instability of the elbow (rotatory external subluxation of the ulna in relation to the humerus) associated with the insufficiency of the lateral ligamentous complex. The clinical picture typically includes painful snapping, clicking, and sometimes locking during extension at 40° of flexion. These symptoms are located in the radial part of the elbow. Although PLRI may be caused by disruption of

the LCL complex, specifically, by secondary insufficiency of the LUCL resulting from trauma [42,43], it may also be due to common extensor tendon diseases [44] or even have an iatrogenic origin [45]. Although the role of magnetic resonance imaging in revealing the anatomical basis of PLRI has been well documented [46], this imaging modality provides only a detailed picture of ligamentous morphology, whereas ultrasonography combines imaging of the morphology of the UCL with dynamic real-time assessment of the pivot shift, which facilitates diagnosis. The part of the LCL that is thought to be of greatest importance in the development of PLRI can be clearly visualized with ultrasonography [47] (◉ Fig. 13).

### Assessment of Degenerative Changes in the Elbow

Synovial hypertrophy, which can be caused by various inflammatory diseases, affects fluid accumulation and synovium formation in the recesses of the elbow [48]. Interposition of thickened, lobulated synovium between the olecranon fossa and the olecranon during extension may cause discomfort and radiating pain in the lateral part of the elbow. Repetitive trauma of

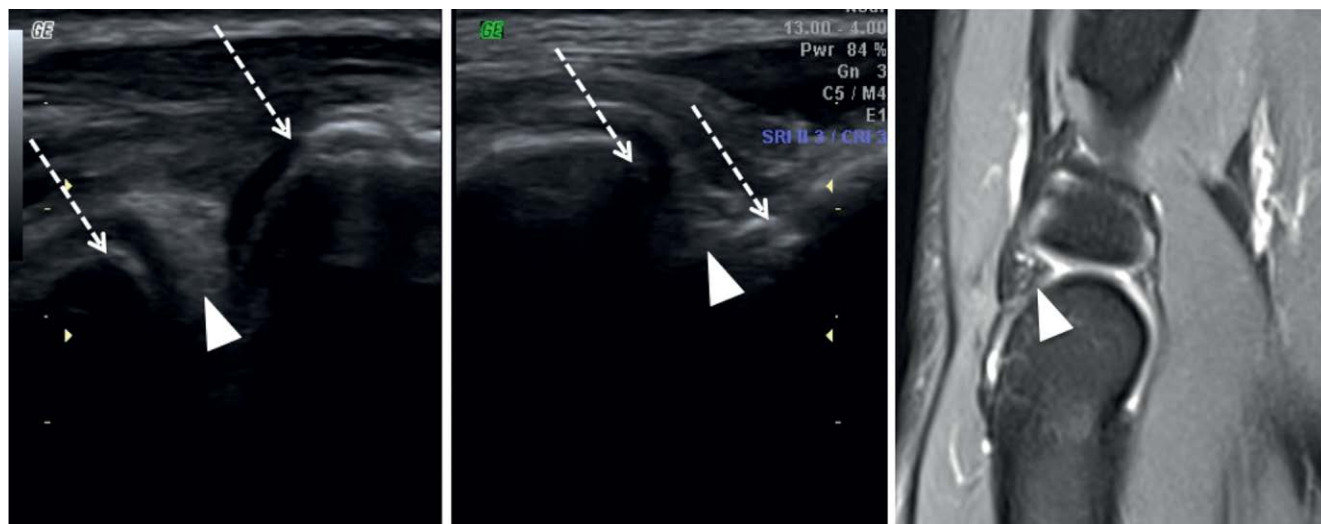


**Fig. 11** Enlarged fibrotic lateral synovial fold of the elbow during a dynamic study: flexion (left) and extension (right). Lateral synovial fold saggital sonograms (linear array probe, 6–12 MHz SP GE [Voluson Expert]) (top). An enlarged fold between the bony capitellum and the radial dome can be observed during flexion, and compression of the fold is visible during extension (bony margins are marked by dashed arrows). The enlarged fold is fibrotic, presenting chronic degenerative changes (arrowheads). Magnetic resonance images (1.5 T Magnetom Essenza) (bottom) of a symptomatic overgrown fold (proton density with fat saturation sequence, sagittal plane).

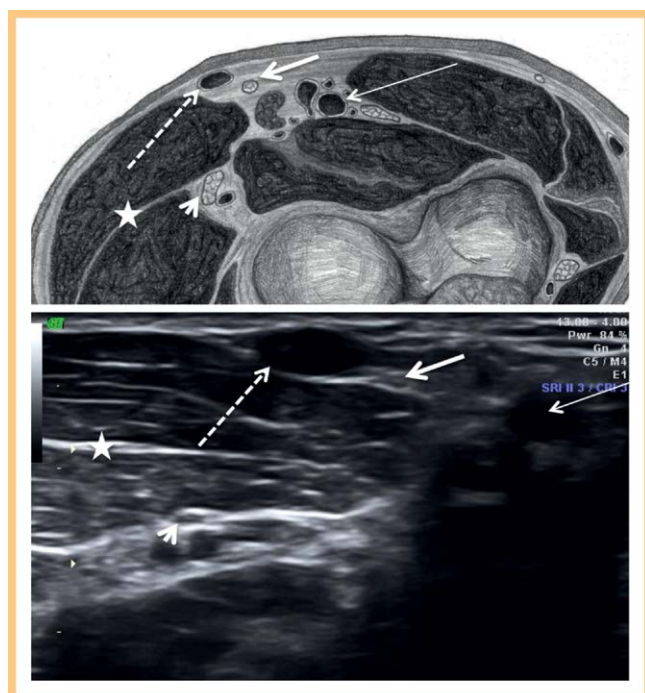


**Fig. 12** Position of lateral antebrachial cutaneous nerve (LABCN) in relation to cephalic vein. Other anatomic structures were marked, Cephalic vein (dashed arrow), LABCN (solid arrow), radial nerve (arrow head), brachial artery (thin solid arrow) and brachioradialis muscle (star). Top, schematic diagram of normal anatomy at the level of proximal elbow. Bottom, corresponding axial sonogram – linear array probe, 6–10 MHz SP GE Voluson 730 Expert.

development of degenerative arthropathy [49]. Real-time ultrasonography can reliably detect the presence of the loose bodies. Furthermore, eventual conflict with bony surfaces during elbow extension can be reliably diagnosed. Ultrasonography can be employed for the evaluation of the severity of arthritis and its precise localization in the lateral elbow [50]. Although lateral elbow pain can be due to synovial hypertrophy in the olecranon fossa alone, it is often caused by inflammation and secondary arthrosis of the radiocapitellar joint. Accordingly, there is a need to detect such potentially symptomatic changes during lateral elbow examination. Irregularity of the bone surfaces, osteophyte formation in the capitellum, and deformation of the radial head (with possible changes to the annular ligament) can all be detected by ultrasonography (► Fig. 14).

### Conclusion

Although lateral elbow pain may be caused by a single pathological factor, as in the case of lateral epicondylitis, the complex anatomy of the region results in possible coexistence of many potentially symptomatic pathologies, all of which must be detected in order to devise an effective treatment approach. Deep knowledge of the anatomy in combination with advanced ultrasonographic skills enables the establishment of accurate differential diagnosis, which is not always possible on the basis of clinical examination alone. Meticulous ultrasonographic examination greatly increases the probability of detection of the causes of lateral elbow pain, whose multifactorial nature should always be taken into account.

the synovium, especially of the olecranon fossa, may lead to its fibrosis. The end stage of the degenerative process is calcification, sometimes resulting in formation of loose bodies. Subsequent interference with the bony parts may provoke the



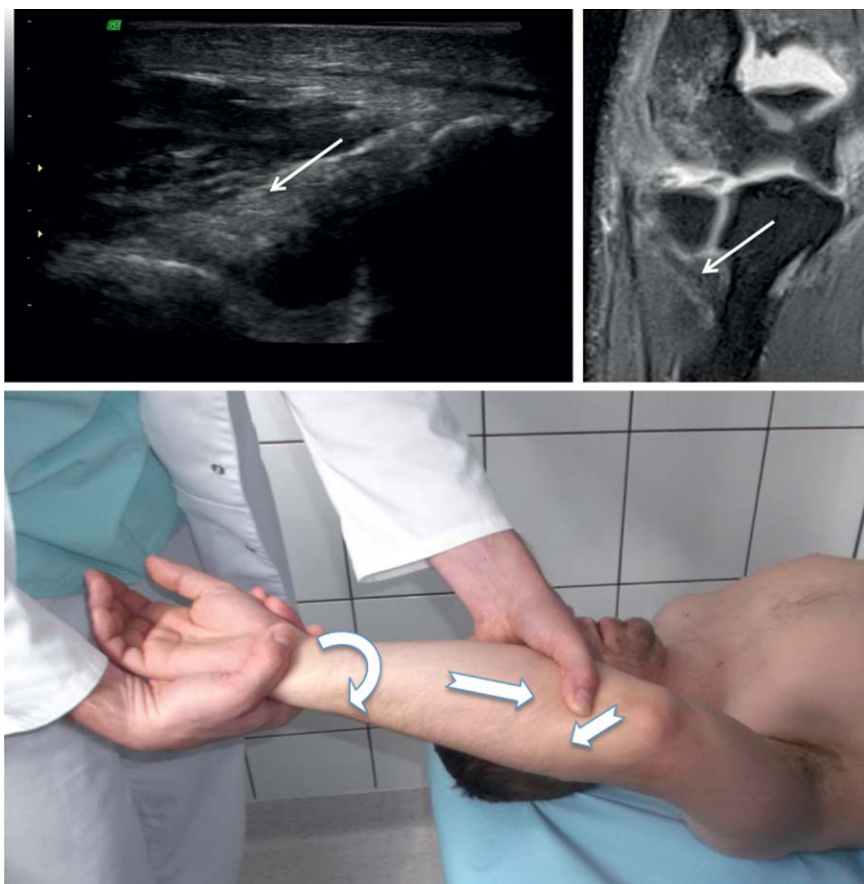


**Fig. 13** Injury of the lateral collateral ulnar ligament caused by posterolateral instability visualized by sonography (left) and magnetic resonance (MR) imaging (right). Sagittal oblique sonograms of the lateral ulnar ligament (linear array probe, 6–12 MHz SP GE [Voluson 730 Expert]) are compared with MR images (proton density fat saturated sequence, coronal plane, 1.5 T Magnetom Essenza). The solid arrows indicate the injured lateral ulnar ligament in the sonogram and the MR image, respectively. Clinical Photograph (below) showing provocative test for lateral ulnar ligament stability assessment – external rotation, axial and valgus loading were applied.

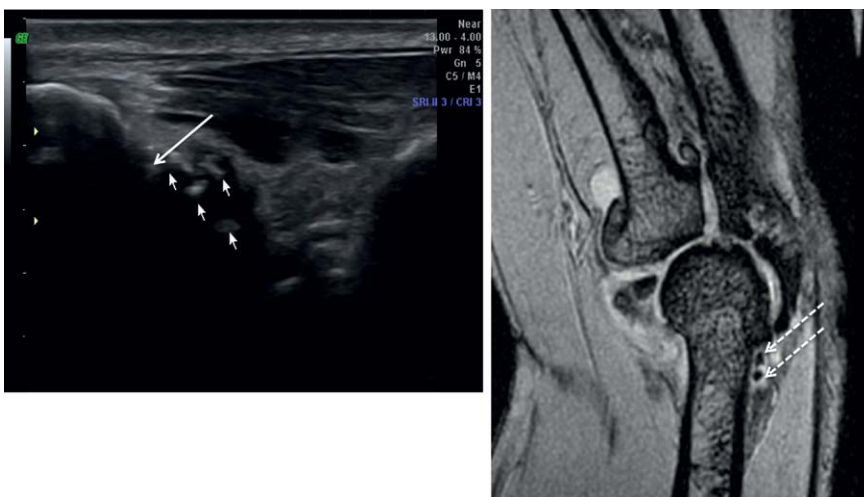


**Fig. 14** Post-inflammatory arthrosis of the elbow joint with posterolateral pain during extension. A sagittal oblique sonogram (linear array probe, 6–12 MHz SP GE [Voluson 730 Expert]) (left), showing the overgrowth of the synovium in the olecranon recess. The image reveals calcification of the synovium (small arrows) as well as irregularities of the bony boundaries of the olecranon fossa (solid arrow). A magnetic resonance image (proton density fat saturated sequence, sagittal plane, 1.5 T Magnetom Essenza) (right) is shown for comparison. The dashed arrows indicate the regions of intrasynovial calcification.

## References

- 1 Clarke AW, Ahmad M, Curtis M et al. Lateral elbow tendinopathy: correlation of ultrasound findings with pain and functional disability. *Am J Sports Med* 2010; 38: 1209–1214
- 2 Plancher KD, Halbrecht J, Lourie GM. Medial and lateral epicondylitis in the athlete. *Clin Sports Med* 1996; 15: 283–305
- 3 Connell D, Burke F, Coombes P et al. Sonographic examination of lateral epicondylitis. *AJR Am J Roentgenol* 2001; 176: 777–782
- 4 Suresh SP, Ali KE, Jones H et al. Medial epicondylitis: is ultrasound guided autologous blood injection an effective treatment? *Br J Sports Med* 2006; 40: 935–939 discussion 939
- 5 Tran N, Chow K. Ultrasonography of the elbow. *Semin Musculoskelet Radiol* 2007; 11: 105–116
- 6 Nazarian LN. The top 10 reasons musculoskeletal sonography is an important complementary or alternative technique to MRI. *AJR Am J Roentgenol* 2008; 190: 1621–1626
- 7 De Smet AA, Winter TC, Best TM et al. Dynamic sonography with valgus stress to assess elbow ulnar collateral ligament injury in baseball pitchers. *Skeletal Radiol* 2002; 31: 671–676
- 8 Bunata RE, Brown DS, Capelo R. Anatomic factors related to the cause of tennis elbow. *J Bone Joint Surg Am* 2007; 89: 1955–1963
- 9 Kraushaar BS, Nirschl RP. Tendinosis of the elbow (tennis elbow). Clinical features and findings of histological, immunohistochemical, and electron microscopy studies. *J Bone Joint Surg Am* 1999; 81: 259–278
- 10 Liu SH, Yang RS, al-Shaikh R et al. Collagen in tendon, ligament, and bone healing. A current review. *Clin Orthop Relat Res* 1995; 318: 265–278
- 11 Kannus P, Józsa L. Histopathological changes preceding spontaneous rupture of a tendon. A controlled study of 891 patients. *J Bone Joint Surg Am* 1991; 73: 1507–1525
- 12 Fenwick SA, Hazleman BL, Riley GP. The vasculature and its role in the damaged and healing tendon. *Arthritis Res* 2002; 4: 252–260



- 13 Levin D, Nazarian LN, Miller TT et al. Lateral epicondylitis of the elbow: US findings. *Radiology* 2005; 237: 230–234
- 14 Martinoli C, Bianchi S, Giovagnorio F et al. Ultrasound of the elbow. *Skeletal Radiol* 2001; 30: 605–614
- 15 Fenwick SA, Hazleman BL, Riley GP. The vasculature and its role in the damaged and healing tendon. *Arthritis Res* 2002; 4: 252–260
- 16 Arirachakaran A, Sukthuyat A, Sisayanarane T et al. Platelet-rich plasma versus autologous blood versus steroid injection in lateral epicondylitis: systematic review and network meta-analysis. *J Orthop Traumatol* 2015
- 17 Ritts GD, Wood MB, Linscheid RL. Radial tunnel syndrome. A ten-year surgical experience. *Clin Orthop Relat Res* 1987; 219: 201–205
- 18 Lin YT, Berger RA, Berger EJ et al. Nerve endings of the wrist joint: a preliminary report of the dorsal radiocarpal ligament. *J Orthop Res* 2006; 24: 1225–1230
- 19 Fuss FK, Wurzl GH. Radial nerve entrapment at the elbow: surgical anatomy. *J Hand Surg Am* 1991; 16: 742–747
- 20 Dang AC, Rodner CM. Unusual compression neuropathies of the forearm, part I: radial nerve. *J Hand Surg Am* 2009; 34: 1906–1914
- 21 Lister GD, Belsole RB, Kleinert HE. The radial tunnel syndrome. *J Hand Surg Am* 1979; 4: 52–59
- 22 Spinner M. The arcade of Frohse and its relationship to posterior interosseous nerve paralysis. *J Bone Joint Surg Br* 1968; 50: 809–812
- 23 Werner CO, Haeffner F, Rosen I. Direct recording of local pressure in the radial tunnel during passive stretch and active contraction of the supinator muscle. *Arch Orthop Trauma Surg* 1980; 96: 299–301
- 24 Djurdjevic T, Loizides A, Löscher W et al. High resolution ultrasound in posterior interosseous nerve syndrome. *Muscle Nerve* 2014; 49: 35–39
- 25 Jelsing EJ, Presley JC, Maida E et al. The effect of magnification on sonographically measured nerve cross-sectional area. *Muscle Nerve* 2015; 51: 30–34
- 26 Dong Q, Jamadar DA, Robertson BL et al. Posterior interosseous nerve of the elbow: normal appearances simulating entrapment. *Ultrasound Med* 2010; 29: 691–696
- 27 Clavert P, Lutz JC, Adam P et al. Frohse's arcade is not the exclusive compression site of the radial nerve in its tunnel. *Orthop Traumatol Surg Res* 2009; 95: 114–118
- 28 Morrey BF, An KN. Functional anatomy of the ligaments of the elbow. *Clin Orthop Relat Res* 1985; 201: 84–90
- 29 Beckett KS, McConnell P, Lagopoulos M et al. Variations in the normal anatomy of the collateral ligaments of the human elbow joint. *J Anat* 2000; 197 (Pt 3): 507–511
- 30 O'Driscoll SW, Bell DF, Morrey BF. Posterolateral rotatory instability of the elbow. *J Bone Joint Surg Am* 1991; 73: 440–446
- 31 O'Driscoll SW, Jupiter JB, King GJ et al. The unstable elbow. *Instr Course Lect* 2001; 50: 89–102
- 32 Miller TT, Adler RS, Friedman L. Sonography of injury of the ulnar collateral ligament of the elbow – initial experience. *Skeletal Radiol* 2004; 33: 386–391
- 33 Akagi M, Nakamura T. Snapping elbow caused by the synovial fold in the radiohumeral joint. *J Shoulder Elbow Surg* 1998; 7: 427–429
- 34 Clarke RP. Symptomatic, lateral synovial fringe (Plica) of the elbow joint. *Arthroscopy* 1988; 4: 112–116
- 35 Isogai S, Murakami G, Wada T et al. Which morphologies of synovial folds result from degeneration and/or aging of the radiohumeral joint: an anatomic study with cadavers and embryos. *J Shoulder Elbow Surg* 2001; 10: 169–181
- 36 Duparc F, Putz R, Michot C et al. The synovial fold of the humeroradial joint: anatomical and histological features, and clinical relevance in lateral epicondylalgia of the elbow. *Surg Radiol Anat* 2002; 24: 302–307
- 37 Bassett FH, Nunley JA. Compression of musculocutaneous nerve at elbow. *J Bone Joint Surg Am* 1982; 64: 1050–1052
- 38 Naam NH, Massoud HA. Painful entrapment of the antebrachial cutaneous nerve at the elbow. *J Hand Surg Am* 2004; 29: 1148–1153
- 39 Rayegani SM, Azadi A. Lateral antebrachial cutaneous nerve injury induced by phlebotomy. *J Brachial Plexus Peripher Nerve Inj* 2007; 2: 6
- 40 Moritz T, Prosch H, Pivec CH et al. High-resolution ultrasound visualization of the subcutaneous nerves of the forearm: a feasibility study in anatomic specimens. *Muscle Nerve* 2014; 49: 676–679
- 41 Tagliafico AS, Michaud J, Marchetti A et al. US imaging of the musculocutaneous nerve. *Skeletal Radiol* 2011; 40: 609–616
- 42 Mehta JA, Bain GI. Posterolateral rotatory instability of the elbow. *J Am Acad Orthop Surg* 2004; 12: 405–415
- 43 Dunning CE, Zarzour ZD, Patterson SD et al. Ligamentous stabilizers against posterolateral rotatory instability of the elbow. *J Bone Joint Surg Am* 2001; 83: 1823–1828
- 44 Dzigan SS, Savoie FH 3rd, Field LD et al. Acute radial ulno-humeral ligament injury in patients with chronic lateral epicondylitis: an observational report. *J Shoulder Elbow Surg* 2012; 21: 1651–1655
- 45 Charalambous CP, Stanley JK. Posterolateral rotatory instability of the elbow. *J Bone Joint Surg Br* 2008; 90: 272–279
- 46 Potter HG, Weiland AJ, Schatz JA et al. Posterolateral rotatory instability of the elbow: usefulness of MR imaging in diagnosis. *Radiology* 1997; 204: 185–189
- 47 Takigawa N, Ryu J, Kish VL et al. Functional anatomy of the lateral collateral ligament complex of the elbow: morphology and strain. *J Hand Surg Br* 2005; 30: 143–147
- 48 De Maeseneer M, Jacobson JA, Jaovisidha S et al. Elbow effusions: distribution of joint fluid with flexion and extension and imaging implications. *Invest Radiol* 1998; 33: 117–125
- 49 Lim YW, van Riet RP, Mittal R et al. Pattern of osteophyte distribution in primary osteoarthritis of the elbow. *J Shoulder Elbow Surg* 2008; 17: 963–966
- 50 Zytoon AA, Eid H, Sakr A et al. Ultrasound assessment of elbow enthesitis in patients with seronegative arthropathies. *J Ultrasound* 2013; 17: 33–40